


Testicular pathology in fatal COVID-19: A descriptive autopsy study

Amaro N. Duarte-Neto^{1,2,*} | Thiago A. Teixeira^{3,*}  | Elia G. Caldini^{1,*} |
 Cristina T. Kanamura² | Michele S. Gomes-Gouvêa⁴ | Angela B. G. dos Santos¹ |
 Renata A. A. Monteiro¹ | João R. R. Pinho⁴ | Thais Mauad¹ | Luiz F. F. da Silva^{1,5} |
 Paulo H. N. Saldiva¹ | Marisa Dolhnikoff¹ | Katia R. M. Leite³ | Jorge Hallak^{1,3}

¹ Departamento de Patologia, Faculdade de Medicina da Universidade de São Paulo, São Paulo, Brazil

² Instituto Adolfo Lutz, São Paulo, Brazil

³ Departamento de Cirurgia, Disciplina de Urologia, Faculdade de Medicina da Universidade de São Paulo, São Paulo, Brazil

⁴ Departamento de Gastroenterologia (LIM-07), Faculdade de Medicina da Universidade de São Paulo, São Paulo, Brazil

⁵ Serviço de Verificação de Óbitos da Capital, Universidade de São Paulo, São Paulo, Brazil

Correspondence

Amaro Nunes Duarte Neto, Faculdade de Medicina da Universidade de São Paulo, Departamento de Patologia, Av. Dr. Arnaldo, 455, sala 1161-Cerqueira Cesar, 01246-903 Sao Paulo, Brazil.
 Email: amaro.ndneto@hc.fm.usp.br

*These authors contributed equally to this work.

Funding Information

Fundação de Amparo à Pesquisa do Estado de São Paulo, Grant Number: 2013/17159-2 (FunderDOI: 10.13039/501100001807); Bill and Melinda Gates Foundation, Grant Number: INV-002396 (FunderDOI: 10.13039/100000865), Fundação Faculdade de Medicina (FFM-FMUSP), Conselho Nacional de Desenvolvimento Científico e Tecnológico, Brazil, Grant Number: 304987/2017-4.

Abstract

Background: Multi-organ damage is a common feature of severe acute respiratory syndrome coronavirus 2 (SARS-CoV-2) infection, going beyond the initially observed severe pneumonia. Evidence that the testis is also compromised is growing.

Objective: To describe the pathological findings in testes from fatal cases of COVID-19, including the detection of viral particles and antigens, and inflammatory cell subsets.

Materials and methods: Postmortem testicular samples were obtained by percutaneous puncture from 11 deceased men and examined by reverse-transcription polymerase chain reaction (RT-PCR) for RNA detection and by light and electron microscopy (EM) for SARS-CoV-2. Immunohistochemistry (IHC) for the SARS-CoV-2 N-protein and lymphocytic and histiocytic markers was also performed.

Results: Eight patients had mild interstitial orchitis, composed mainly of CD68+ and TCD8+ cells. Fibrin thrombi were detected in five cases. All cases presented congestion, interstitial edema, thickening of the tubular basal membrane, decreased Leydig and Sertoli cells with reduced spermatogenesis, and strong expression of vascular cell adhesion molecule (VCAM) in vessels. IHC detected SARS-Cov-2 antigen in Leydig cells, Sertoli cells, spermatogonia, and fibroblasts in all cases. EM detected viral particles in the cytoplasm of fibroblasts, endothelium, Sertoli and Leydig cells, spermatids, and epithelial cells of the rete testis in four cases, while RT-PCR detected SARS-CoV-2 RNA in three cases.

Discussion and conclusion: The COVID-19-associated testicular lesion revealed a combination of orchitis, vascular changes, basal membrane thickening, Leydig and Sertoli cell scarcity, and reduced spermatogenesis associated with SARS-CoV-2 local infection that may impair hormonal function and fertility in men.

KEYWORDS

autopsy, COVID-19, Leydig cell, orchitis, SARS-CoV-2, testis

1 | INTRODUCTION

The severe acute respiratory syndrome-coronavirus 2 (SARS-CoV-2) is a recently-emerged coronavirus that was first reported in late 2019 at the Chinese city of Wuhan and is the causative agent of the new and mostly unknown pandemic disease, COVID-19, with a wide variety of implications in human health.^{1,2} Compared to the previously described beta coronavirus, this new entity spreads strategically in silence for more extended periods before patients become clinically symptomatic and the virus is eventually identified.³ By April 15th, 2021, the pandemic had affected almost 140 million cases and caused close to three million deaths, with the USA, India, Brazil, France, and Russia, as the five countries with the highest number of cases.⁴

COVID-19 manifests mainly by respiratory symptoms.^{1,2} However, as the pandemic progresses, this paradigm has changed as cumulative evidence has shown that COVID-19 is a systemic condition.⁵ Therefore, understanding multiple organ involvement is crucial to fully comprehend COVID-19 pathophysiology.^{3,6} It is believed that systemic involvement occurs because of the presence of angiotensin-converting enzyme 2 (ACE2), the cell surface receptor for SARS-CoV-2, and transmembrane serine protease 2 (TMPRSS2), responsible for priming the viral S protein to facilitate viral entry, in several organs and tissues. Recognizing the expression of these proteins throughout the human body is essential to understand the clinical manifestations and predict potential lesions in organs that are often overlooked.⁷

SARS-CoV-2 infection of the male reproductive tract (MRT) has gained interest as the male gender has the highest number of cases and the highest risk of severe COVID-19, including hospitalization rates in intensive care units and a high proportion of cases with unfavorable outcomes.^{8,9} The testes have the highest ACE2 expression in the human body, according to data from the Genotype-Tissue Expression Project,¹⁰ and this receptor is primarily found in spermatogonia, Leydig, and Sertoli cells.¹¹ Theoretically, this fact renders testicles highly susceptible to SARS-CoV-2 infection and damage, and, therefore, male COVID-19 patients are prone to develop testicular morphofunctional changes.¹² It remains unclear whether these potential alterations can translate into prolonged or even permanent damage, negatively impacting the fertility status or establishing an early-onset hormonal imbalance.^{12–15}

The COVID-19 pandemic in Brazil began on February 26th, 2020. By April 15th, 2021, more than 13.5 million confirmed cases had been registered, with more than 350 thousand deaths. The male/female ratios of SARS cases and deaths from COVID-19 in Brazil are 1.27 and 1.35, respectively.⁴ Since the start of the pandemic, our institution was designated by the São Paulo state health department as the public referral hospital to treat severe cases. From March 30th to October 3rd, 2020, over 4000 confirmed cases of COVID-19 were admitted to the hospital, with 1400 deaths (fatality rate, 34.9%).

We have previously described the autopsy findings on our first ten fatal cases of COVID-19 (including five male patients), in which we found signs of orchitis in the two testicle samples obtained through a percutaneous puncture.¹⁶ The present study aims to detail the histological description of SARS-CoV-2-related testicular damage and

investigate viral particles and antigens in the lesions by immunohistochemistry (IHC), reverse-transcription polymerase chain reaction (RT-PCR), and electron microscopy (EM), in a greater number of testicular samples from fatal cases of COVID-19.

2 | MATERIALS AND METHODS

The HC-FMUSP Ethical Committee approved this research (protocol no. 3951.904), which was performed according to the Declaration of Helsinki. Confirmed cases of COVID-19 were defined according to the World Health Organization (WHO) as those with laboratory confirmation of SARS-CoV-2 infection, regardless of clinical signs and symptoms (Table 1).

From March 18th to May 15th, we autopsied 41 COVID-19 deceased patients, of whom 22 were male. Eleven testes' samples were obtained, mainly from the tubular parenchyma, with two cases including the *rete testis*. In eight cases, we did not collect testicular samples, and in three cases, the sample did not represent the testicular parenchyma.

The autopsy was performed after written consent from the next-of-kin as previously described.¹⁶ Ultrasound-guided minimally invasive autopsy (MIA-US) was employed to examine and guide tissue sampling, using Tru-Cut semi-automatic coaxial needles (14G). The testicular samples (at least two fragments from each patient, one for each side) were obtained by a transcutaneous puncture. Tissue samples were routinely processed, and paraffin sections (3–5 μm) were stained with hematoxylin-eosin and Masson's trichrome. All cases were analyzed under a light microscope by pathologists with extensive autopsy experience (Amaro N. Duarte-Neto, Marisa Dolhnikoff, Paulo H. N. Saldiva, Thais Mauad, Luiz F. F. da Silva) and by a uropathologist (Katia R. M. Leite). The following histological parameters were analyzed: interstitial edema, inflammatory infiltrate, vascular changes (congestion, endothelial tumefaction, thrombi, vasculitis, ischemic infarction), basal membrane thickness and peritubular fibrosis (total or partial), tubular atrophy (focal in isolated microscopic fields or diffuse throughout the sample), germ cell aspect, spermatogenesis (normal or decreased, when full spermatogenesis was not observed within tubules), and Leydig cell aspect (number and disarray). The Leydig cell number was considered diminished when groups of less than five interstitial cells were observed in several fields (200x amplification).

IHC of testicular tissue was performed in all cases to detect the SARS-COV-2 nucleocapsid antigen using a mouse monoclonal antibody [6H3] (GeneTex Inc., Irvine, CA, USA; 1:2000 dilution), and the expression of ACE2 (ABCAM, ab65863, Cambridge, UK, Rabbit; 1:2500 dilution), TMPRSS2 (ABCAM, EPR3862; 1:3000 dilution), D68 (DAKO, Via Real Carpinteria, CA, USA, PG-M1; 1:2500 dilution), CD57 (DAKO, TB01; 1:200 dilution), CD4 (Leica-Novocastra, Buffalo Grove, IL, USA, 4B12; 1:150 dilution), CD8 (DAKO, C8144B; 1:400 dilution), CD20 (DAKO, L26; 1:2500 dilution), TGF- β -1 (Santa Cruz, Dallas, TX, USA, TB21; 1:150 dilution), and VCAM (Santa Cruz, E-10; 1:100 dilution). All the antigen retrievals were performed with citrate at pH 6.0, except for CD68 antigen detection, which was done using

TABLE 1

Case number	Age (years)	S-D; H (days)	Comorbidities	COVID-19 diagnosis	Lung pathology	Orchitis	Vessels	Tubular fibrosis	Spermatogenesis	Testis tissue	CD68	CD20	CD4	CD8	CD57	RT-PCR-SARS-CoV-2
1	79	11;9	DM, SAH, Cardiopathy, Stroke, CKD, COPD, Tobacco	N/O swab	Pt, thrombi in skin, kidney COVID-19 pn	+	Endothelial swelling, ectasia	Partial thickening	Normal	NA	+	0	+	+	+	NA
2	59	16;11	DM, Cardiopathy, ex-Tobacco	Clinical features, Tomography, histology, and IH+ (lungs)	Pt, secondary pneumonia COVID-19 pn	+	Endothelial swelling	Focal atrophy	↓	NA	++	0	+	+	+	NA
3	88	12;7	None	RT-PCRLung	Pt COVID-19 pn	+	Endothelial swelling, ectasia, fibrin thrombi, organized thrombus	Focal atrophy	Normal	NA	++	+	+	++	+	NA
4 ^{†,§}	41	26;21	SAH	RT-PCRTracheal	Pt, secondary pneumonia COVID-19 pn	+	–	Partial thickening	↓	Not detected	+	0	+	+	+	Not detected
5§	66	7;4	SAH, Cardiopathy, ex-Tobacco	RT-PCRLung	Pt, secondary pneumonia COVID-19 pn	+	Endothelial swelling, Fibrin	Partial thickening	↓	Detected	++	0	+	0	+	Detected
6 [§]	51	31;14	None	N/O swab	Pt, secondary pneumonia COVID-19 pn	–	Endothelial swelling, PMN margination	Focal atrophy	↓	Not detected	++	0	+	+	+	Not detected
7	67	10;3	SAH, Cardiopathy, ex-Tobacco	N/O swab	COVID-19 pn	–	Endothelial swelling	Focal atrophy	Normal	Detected	+	0	+	+	+	Detected

(Continues)

TABLE 1 (Continued)

Case number	Age (years)	S-D; H (days)	Comorbidities	COVID-19 diagnosis	Lung pathology	Orchitis	Vessels	Tubular fibrosis	Spermatogenesis	RT-PCR-SARS-CoV-2 Testis tissue	CD68	CD20	CD4	CD8	CD57
8	64	14;12	DM, SAH	RT-PCR Lung	Pt, secondary pneumonia	-	Endothelial swelling	Partial thickening	Normal	Detected	+	0	+	+	+
9	45	20;15	DM, SAH, CKD	N/O swab	PtCOVID-19 pn	+	Endothelial swelling, Fibrin	Focal atrophy	Normal	Not detected	++	+	+	+	+
10	32	32;26	Naguille smoking	N/O swab	Secondary pneumoniaCOVID-19 pn	+	Endothelial swelling, thrombi	Focal atrophy	↓↓↓	Not detected	+++	0	+	+	+
11 ^{* §}	65	32;20	Cannabis smoking	N/O swab	COVID-19 pn	+	Endothelial swelling, thrombi	Focal atrophy	↓	NA	+	0	+	+	+

Abbreviations: CKD, chronic kidney disease; COVID-19 pn, COVID-19 typical pneumonia; DM, diabetes mellitus; H, in-hospital stay; Pt, pulmonary thromboembolism; RT-PCR, reverse polymerase chain reaction; SAH, systemic arterial hypertension; S-D, time from symptoms onset to death.

[†]SARS-CoV-2 Pango lineage B.1.1.28 in Brazil, circulating in 2020.

*Cases with rete testis sampling.

§Cases with electron microscopy analysis.

COVID-19 typical pneumonia: cytopathic effect on alveolar epithelial cells; diffuse alveolar damage (alveolar edema, hyaline membrane, and fibroproliferative changes); mild inflammatory response.

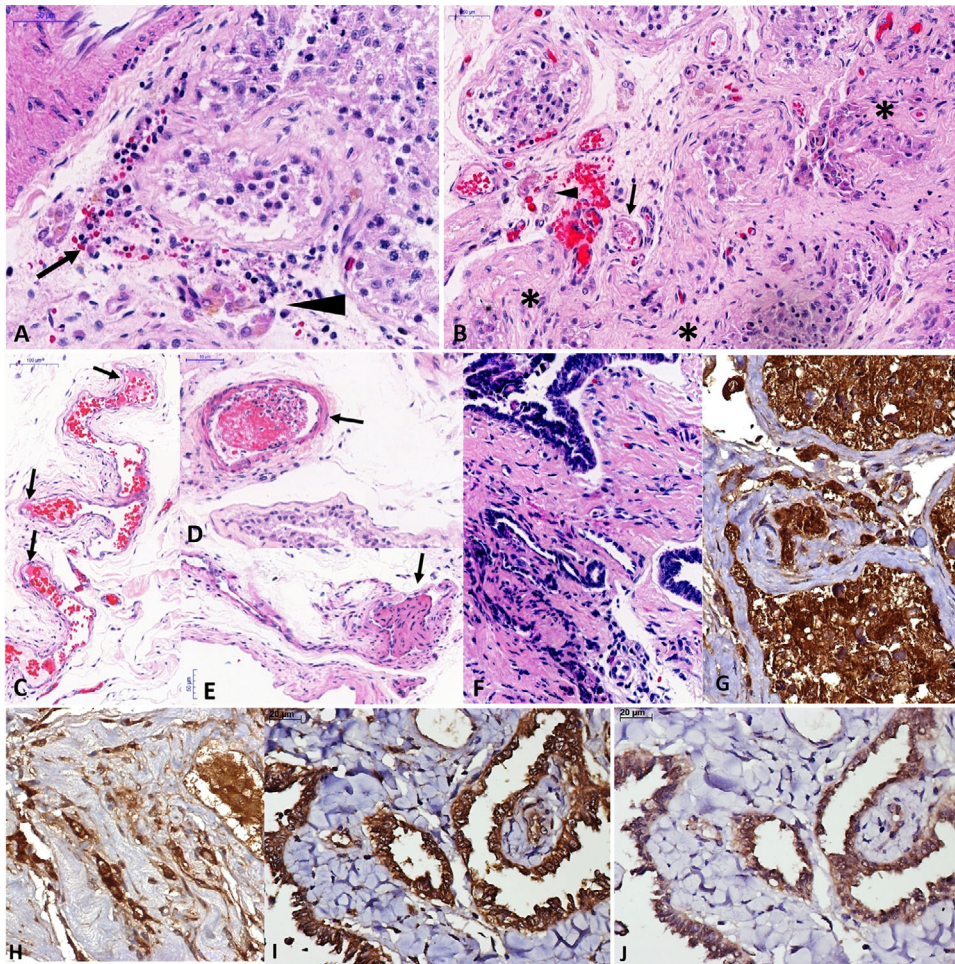


FIGURE 1 Pathological findings in testes from fatal cases of COVID-19. (A) Interstitial orchitis, with mononuclear inflammatory cells (arrow), interstitial edema and disarrangement of Leydig cells (arrowhead), and decreased spermatogenesis in a patient with 45 years old and 20 days of disease duration. (B) Atrophic tubules (asterisks), fibrin thrombus within the small artery (arrow), and Leydig cell disarrangement (arrowhead) in the same patient from A. (C) Endothelial swelling and fibrin within a testicular vein. (D) Recent thrombi in a testicular artery. (E) Organized thrombus in a testicular vein. (F) Interstitial inflammation in rete testis in a patient 41 years old. (G–J) The expression of angiotensin-converting enzyme 2 (ACE-2) is seen in Sertoli cells, spermatogonia, fibroblasts, and Leydig cells in young adults with (G) preserved tubules (G) and (H) atrophic tubules. The expressions of (I) ACE-2 and (J) transmembrane serine protease 2 (TMPRSS2) are coincident in rete testis, as well as in testes

TRIS-EDTA at pH 9.0. The reactions followed standard protocols validated in our laboratories, using positive (paraffin-embedded lung samples from COVID-19 fatal cases) and negative controls (testes from patients with cardiovascular diseases, diabetes, mumps, measles, yellow fever, dengue, and HIV infection).

We performed a semi-quantitative analysis of the tissue content of immune cells as follows: (0) absence, (+) occasional cells in distant high-power fields (HPFs) (separated by at least two HPFs), (++) occasional cells in adjacent HPFs, and (+++) various cells in adjacent HPFs.

Fresh testicular tissue samples from six cases were stored at -80°C for SARS-CoV-2 molecular detection by real-time RT-PCR (rRT-PCR) using the SuperScriptTM III PlatinumTM One-Step qRT-PCR Kit (Invitrogen, Waltham, MA, USA) and primers and probes that amplify the region of the nucleocapsid N (CDC protocol) and E genes.^{17,18} The human RNase P gene (*RP*) was also amplified as a nucleic acid extraction control. The reactions were carried out in a 7500 Fast Real-Time PCR System (Applied Biosystems, Waltham, MA, USA) using

the following thermal conditions: incubation at 50°C for 15 min for the reverse transcription, followed by incubation at 95°C for 2 min, and 45 cycles of temperature varying from 95°C for 15 s to 55°C for 30 s.

In four cases (cases 4, 5, 6, and 11), paraffin-embedded tissue samples were examined under a transmission electron microscope (EM) (JEM 1010; JEOL, Tokyo, Japan, 80 kV) by a specialist (Elia G. Caldini). We reprocessed the paraffin-embedded biological tissue for EM, selecting a specific area from the block with positive IHC labeling for the SARS-CoV-2 N-protein (see Figure 2). The target areas were dug out using a razor blade, and then the fragments were deparaffinized in xylol, rehydrated in a graded alcohol series, and re-fixed with glutaraldehyde in 0.15 M phosphate buffer, followed by post-fixation in 1% OsO_4 , and staining in 1% aqueous uranyl acetate overnight. Next, the specimens were embedded in epoxy resin. Ultrathin sections were obtained with a Reichert ultratome and double-stained with uranyl acetate and lead citrate.

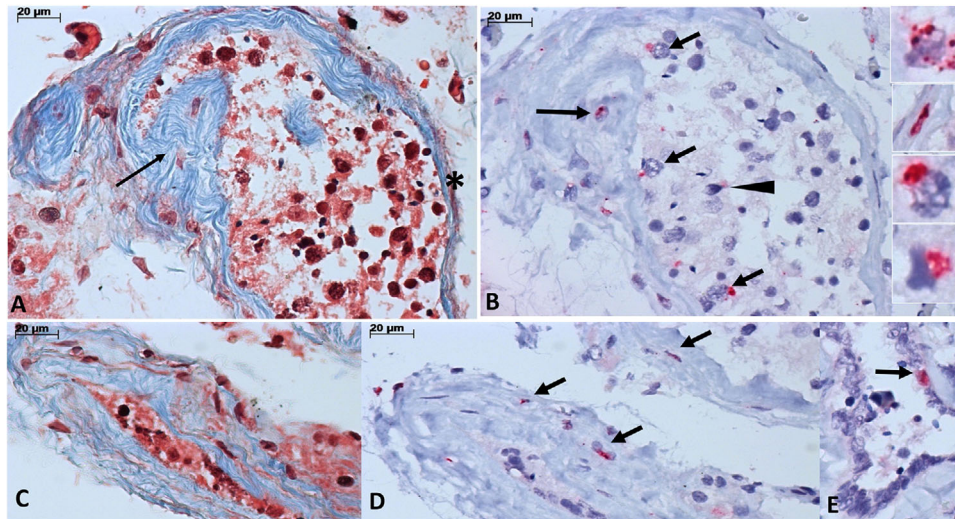


FIGURE 2 Severe acute respiratory syndrome coronavirus 2 (SARS-CoV-2) N-antigen detection in testes from fatal cases of COVID-19. (A) Tubule with partial fibrotic thickening of the basal membrane (arrow) and area of thinner basal membrane (asterisk) (Masson's trichrome). (B) The same tubule is shown in (A), with positive detection of SARS-CoV-2 N-protein by immunohistochemistry [IHC] in fibroblasts in the basal membrane (long arrow), Sertoli cells (small arrows), and spermatogonia (arrowhead). The insets, from top to bottom, show immunostaining in the cytoplasm of a Leydig cell, fibroblast, Sertoli cell, and spermatogonia. (C, D) An atrophic tubule (C, Masson's trichrome) with positive immunostaining for SARS-CoV-2 N-protein in the cytoplasm of fibroblast from the basal membrane (D, IHC). (E) Positive detection of SARS-CoV-2 N-protein in the cytoplasm of epithelial cell from the rete testis (E, IHC)

3 | RESULTS

3.1 | Subjects, clinical findings, and overview of autopsy results

The 11 patients had the following characteristics (Table 1): median age of 64 (range, 32–88) years, body mass index (BMI) of 24.2 (range, 20.4–29.4) kg/m², disease duration of 16 (range, 7–32) days, and hospital stay length of 12 (range, 3–26) days. The most prevalent comorbidities were systemic arterial hypertension (six cases), diabetes mellitus (four cases), and cardiopathy (four cases). Four patients informed about tobacco use. The main clinical symptoms were fever (nine cases), dyspnea (eight cases), cough (seven cases), and diarrhea (five cases). No patient reported testicular pain or scrotum enlargement.

The median concentration of the D-dimer was 3132.5 (range, 815–84,864 [Reference value ≤ 500 ng/ml]) and of C-reactive protein, 271.55 (range, 71.7–351.4 [reference value < 5 mg/L]). No patient received hydroxychloroquine, ivermectin, or prednisone. Two patients received methylprednisolone and three, hydrocortisone. Six patients received anticoagulant therapy. Death in all patients was due to refractory hypoxemia, mixed acidosis, renal failure, and severe cardiac dysfunction.

The lung samples obtained by MIA-US demonstrated typical SARS-CoV-2 pneumonia, with intense cytopathic effects on pneumocytes and diffuse alveolar damage in the exudative and fibroproliferative phases. Thrombi in pulmonary vessels were seen in eight cases (73%). Secondary pneumonia with associated suppurative infiltrate was seen in six cases.

3.2 | Microscopic and molecular analyses of the testes

Eight cases (73%) presented orchitis, characterized by a mild-to-moderate interstitial and mononuclear inflammatory infiltrate, composed mainly of CD68+ cells and a few TCD8+ cells. Few TCD4+ and CD57+ cells were found, and CD20+ cells were rare. No inflammatory cells were observed within the tubules, or vasculitis (Table 1 and Figures 1A and B, Figure 4). Interstitial edema was pronounced in all cases. Vascular changes (congestion, endothelial tumefaction, fibrin thrombi, or organized thrombi) were also present in all cases (Table 1 and Figure 1C–E). Leydig cells were reduced and disarranged in all samples (Figure 1A and B). Focal tubular atrophy was present in seven cases and partial tubular thickening in three (Figure 1A and B, Figure 2). Sertoli cells showed detachment from the basement membrane, and spermatogonia were sloughed in the tubular lumen (Figure 1B). A decrease in spermatogenesis was observed in six cases. Interstitial apoptotic cells were not found by H&E and EM analysis.

The SARS-CoV-2 N-capsid protein was detected in all cases in Leydig cells, Sertoli cells, spermatogonia, and fibroblasts (Figure 2A–E). No case was positive for the SARS-CoV-2 N-antigen on spermatozoa or endothelial cells. SARS-CoV-2 RNA was detected by rRT-PCR in 50% (3/6) of testicular tissue samples. EM (Figure 3) revealed viral particles (50–100 nm in diameter) in the cytoplasm of interstitial cells (Leydig cells and fibroblasts), Sertoli cells, spermatid, endothelial cells (rare cells) in all four cases, and within epithelial cells from *rete testis* in one case (case 5).

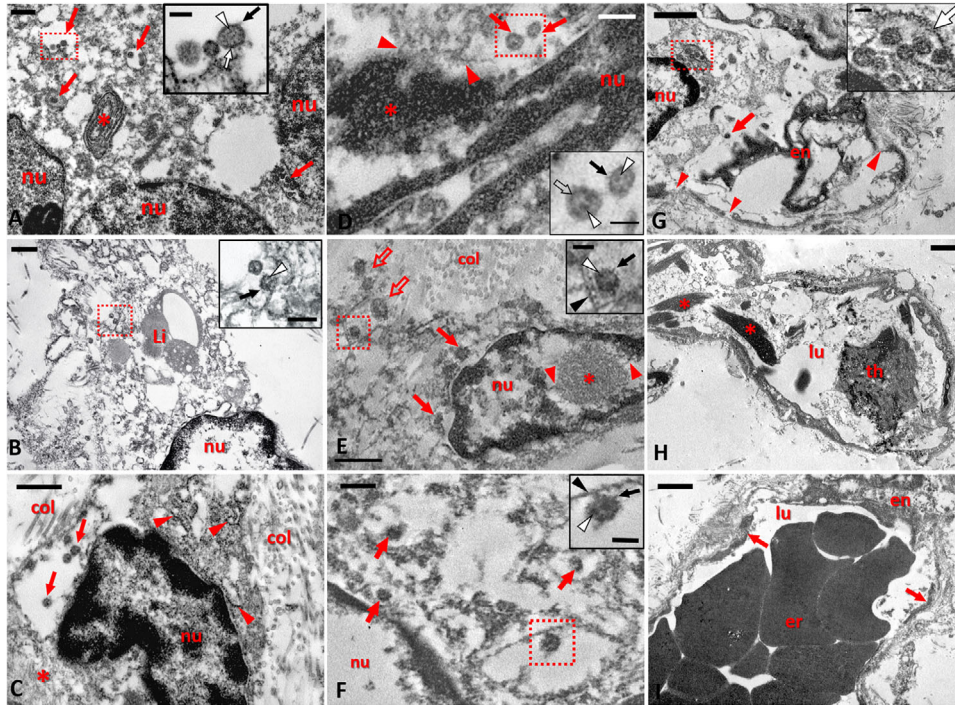


FIGURE 3 Testicular electron microscopy findings in a fatal case of COVID-19. (A) High magnification electron micrograph (EM) of the seminiferous epithelium showing parts of three spermatids typically united (nu: nucleus). The presence of rough endoplasmic reticulum (asterisk) denotes the synthetic activity of the cells. Note the cytoplasmic vesiculation and the presence of viral particles in some of them (arrows). The inset corresponds to a higher magnification of the vesicle in the boxed area with three viral particles. Note the viral envelope (white arrow), nucleocapsids (white arrowhead), and spikes (black arrow) at the virus particle surface. (B) EM of part of a virus-infected Leydig cell (nu: nucleus; Li: lipid inclusions). The cytoplasm shows vesiculation, which is typical of coronavirus infection. The boxed area corresponds to an intracytoplasmic vesicle containing two viral particles circa 100 nm in diameter. Inset shows a higher magnification of the virions with electron-dense dots resembling nucleocapsids (white arrowhead) particles and spike-like surface projections (black arrow). (C) EM of a representative myofibroblast in the testis interstitium (nu: nucleus) presenting the typical features, mainly, abundant rough endoplasmic reticulum (arrowheads) and smooth-muscle actin filaments (asterisk). In the supranuclear position, there is a big membrane-bounded vesicle containing virus particles (arrows), col: collagen fibrils. (D) EM evidences viral (arrows) particles (circa 100 nm in diameter), near to nucleus (nu) of a Sertoli cell. Note the presence of threads of extranuclear chromatin (arrowheads) released from a nuclear zone of decondensed chromatin (asterisk). Inset corresponds to a higher magnification of viral particles showing typical coronavirus characteristics: electron-dense dots resembling nucleocapsids (white arrowheads) within the virus particle, surface projections (spikes, black arrow), and a membrane envelope (open arrow). (E) EM of a cell in the interstitial connective tissue of testes showing coronavirus particles present in both intracellular (arrows) and extracellular (open arrows) locations, col: collagen fibrils. Part of the nucleus (nu) is occupied by the mesh-like structure of decondensed chromatin fibers (asterisk). The arrowheads highlight that these chromatin fibers are continuous with those of the heterochromatin. Inset corresponds to a higher magnification of a coronavirus particle showing nucleocapsids (white arrowhead) and surface projections resembling spikes (black arrow). Note that the SARS-CoV-2 particle is located within a membrane compartment (black arrowhead) typically attached to the inner membrane surface. (F) Rete testis epithelial cells showing part of the nucleus (nu) and the cytoplasm containing coronavirus particles (arrows) inside vesicular compartments. Inset corresponds to a higher magnification of a viral-like particle attached to the vesicular membrane (black arrowhead). Note nucleocapsids (white arrowhead) and spikes at virus surface (black arrow). (G) EM of a virus-infected cell (n: nucleus) inside the lumen of a capillary of the testis interstitium. The inset image corresponds to a higher magnification of the area surrounded by dotted lines showing some viral particles within a membrane-bounded vacuole (white arrow). The cytoplasm presents fragmented areas and it is possible to observe a virus particle-free (arrow) in the capillary lumen. The endothelial cell (en) is detached from the basal membrane and some areas of vascular are wall ruptured (arrowheads). (H) Low magnification EM of a representative blood capillary found in the testis interstitium. The vascular lumen (lu) is filled by cellular debris, bundles of fibrin fibers (asterisks), and an organized microthrombus (th). (I) Low magnification EM of an enlarged capillary of the testis interstitium. The lumen (lu) was full of aggregated erythrocytes (er). The endothelial layer (en) is damaged or absent, while fibrin deposits (arrows) are found adjacent to the basement membrane. These electron microscopy results corroborate the immunohistochemical findings (SARS-CoV-2 N-antigen detection) in the testicular samples.

Magnifications (Bar scales): A, 500 nm; B, 500 nm; C, 500 nm; D, 200 nm; E, 500 nm; F, 200 nm; G, H, and I, 1000 nm; Inset, 100 nm, except B (200 nm); EM, electron micrograph

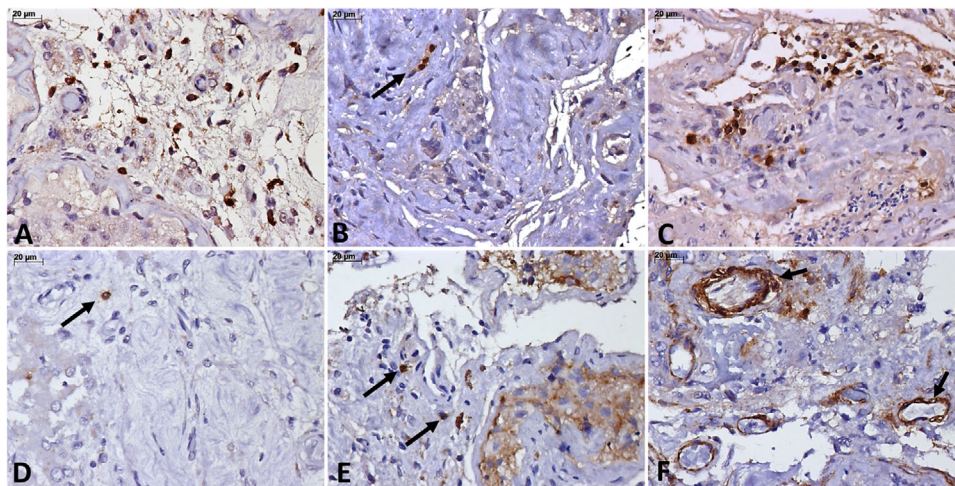


FIGURE 4 Pathological aspects in the COVID-19 related orchitis, from cases with fatal outcome. (A-E) Testicular inflammatory infiltrate is composed of a moderate number of CD-68+ cells (A), scarce TCD-4+ cells (B), a moderate number of TCD-8+ cells (C), rare CD-20+ cells (D), and CD-57+ cells (E). (F) Strong expression of vascular cell adhesion molecule (VCAM) in testicular vessels (arrows). Peroxidase, 400 \times , scale bars: 20 μ m

Expression of TGF- β -1 was not detected in mesenchymal cells or interstitial inflammatory cells. ACE2 and TMPRSS2 expression was present in all cases, regardless of age, and these two immune stains were simultaneously present in the same cells (Leydig cells, Sertoli cells, spermatogonia, endothelium, and fibroblasts). Even atrophic tubules co-expressed ACE2 and TMPRSS2 (Figure 1G–J).

4 | DISCUSSION

We previously reported orchitis in two fatal cases of COVID-19 at the beginning of the epidemic in São Paulo state, Brazil.¹⁶ As the epidemic progressed and the number of autopsies increased, the testicular findings in fatal cases of COVID-19 remained frequent, and we now present the results of a more significant number of cases.

The present study shows that there are testicular lesions in patients with fatal COVID-19, which can be attributed to inflammatory changes associated with SARS-CoV-2 in the testicular parenchyma and to varying degrees of vascular damage with secondary ischemia.

SARS-CoV acts as an archetype for the COVID-19 testicular pathophysiological hypothesis because it shares exactly the same cell invasion mechanism.¹⁹ During the SARS-2005 epidemic in China, Xu et al. described testicular lesions in six deceased men: orchitis, germ cell damage, presence of scarce or no spermatozoa in the seminiferous tubules, basement membrane thickening, peritubular fibrosis, interstitial vascular congestion, leukocyte infiltration, and decrease in Leydig cells were the main findings.²⁰ We found similar testicular lesions in our cases, which other authors have also observed.^{21–24}

Orchitis was found in 73% of our cases, but this rate may be higher since the inflammation is focal and may have been underestimated in the samples obtained percutaneously, given their small size. Interstitial orchitis was mild, composed mainly of macrophages, with lower

participation of other cell types. This profile was also found by other authors,^{21–24} but the presence of CD8 + cells in ten of our cases suggests that cytotoxicity plays a relevant role in SARS-CoV-2 orchitis.

SARS-Cov-2 was detected in testicular tissue by IHC, EM, and through detection of viral RNA by rRT-PCR. IHC was positive in Leydig cells, Sertoli cells, spermatogonia, and fibroblasts in all cases, even in those with more than 30 days of disease (see Table 1 and Figure 2A–E). This result suggests that the clearance of viral antigens in the testis can take a long time, possibly inducing severe cellular changes (for example, loss of Leydig cells due to viral infection). The clinical repercussions of these findings still need to be elucidated. EM confirmed the detection of viral particles in several cell types, including Leydig cells, fibroblasts, endothelial cells, spermatid, Sertoli cells, and the epithelium of the *rete testis*. This finding is corroborated by the works of Ma et al.²² and Achua et al.,²¹ where the authors demonstrated SARS-CoV-2 particles in interstitial cells. Since we collected samples from paraffin blocks, guided by the areas with the greatest IHC labeling for the SARS-CoV-2 N-protein, this strategy probably favored the detection of viral particles in multiple testicular cell types.

Two other pathological changes were relevant in our series: the thickening of the seminiferous tubule basal membrane and vascular changes. Basal membrane thickening was observed in all cases through Masson's trichrome staining in tubules with complete or partial atrophy. Interestingly, the areas with basal membrane thickening revealed fibroblasts positively immunolabeled for the SARS-CoV-2 N protein and viral particles by EM, suggesting that fibroblast infection may trigger the deposition of extracellular matrix in the seminiferous tubules (Figures 2A–D, Figure 3C). Further studies are needed to understand if this alteration can progress to complete atrophy, potentially associated with infertility, or if it is reversible over time. TGF- β -1 expression was negative in all samples, suggesting that collagen deposition in the basal membrane does not seem to be mediated by this pathway.

Vascular changes in the testicular tissue of patients with COVID-19 have not been previously described. In our patients, alterations included congestion and endothelial swelling, present in all cases, and fibrinous thrombi in five cases, one of which with venous thrombus organization. The EM detected rare endothelial cells with viral particles, which explains the non-expression of viral N-antigen in these cells by IHC. This result suggests that viral-induced endothelial changes were not the primary mechanism of the thrombotic changes. We attribute the testicular vascular changes mainly to COVID-19-related systemic alterations, such as refractory hypoxemia, multi-systemic thrombosis, and secondary infections. Testicular ischemia due to shock and thrombosis is likely to be responsible for decreasing spermatogenesis and detachment of tubular cells from the basal membrane²⁵ as observed in our patients and by others.²⁰⁻²³ We did not find inflammatory cell exocytosis into the tubular epithelium, despite viral antigen labeling of Sertoli cells and spermatogonia.

Some viral types are known to directly infect the testes or induce a systemic inflammatory response, with indirect effects on testicular function, impairing male fertility to different degrees.²⁶

The mumps virus (MuV) is the prototype of an agent that causes testicular damage. The MuV-related orchitis presents congestion, interstitial edema, lymphocytic infiltration, seminiferous tubule congestion, tubular hyalinization, germinal epithelium atrophy, and fibrosis.^{27,28} In the MuV orchitis, germ cell apoptosis can be induced by the C-X-C motif chemokine ligand 10 produced by infected Sertoli cells, and spermatogenesis impairment is observed due to paracrine dysregulation by macrophages, Sertoli, and Leydig cells.²⁹

Based on autopsy studies, HIV-1 causes a myriad of testicular damages, including germ cell loss, perivasculitis, lymphocytic infiltration, interstitial fibrosis, basement membrane thickening, testicular atrophy, and the "Sertoli-cell-only" syndrome, the most common testicular change found in this infection (43%).³⁰

The testis is a primary target of the Zika virus (ZIKV), acting as an anatomic reservoir with high viral loads, even over prolonged periods.³¹⁻³³ ZIKV can replicate in human germ cells *in vivo* and in all testis explant components, such as in macrophages, peritubular, Sertoli, and Leydig cells.^{31,34} No significant histological lesion has been described in the testes of ZIKV-infected patients, although viral RNA can be found in the epididymis, vas deferens, and seminal vesicles.^{31,35,36} The yellow fever virus, another flavivirus, can also produce orchitis.³⁷

Like ZIKV, the Filoviridae family also uses the testes as an immune-privileged niche for persistence in male survivors.^{38,39} The Filoviridae family members, Ebola virus and Marburg virus, can cause fatal hemorrhagic fever. Autopsy studies have described necrotic orchitis in Marburg virus infection^{39,40} and Ebola virus antigens in testicular endothelial cells and seminiferous tubules.⁴¹ In chronic hepatitis B infection, the viral target cells in the testicular tissue are the intertubular stromal fibroblasts and endothelial cells.⁴² Other viruses may also induce orchitis, primarily systemically, including dengue, coxsackie, rubella, echovirus, and influenza viruses.²⁶

As mentioned, testicular changes in COVID-19 are similar to those observed in SARS²⁰; inflammatory changes that decrease spermatogenesis and hormonal production due to Leydig cell loss.

The works of Yang et al.,²³ Achua et al.,²¹ and Ma et al.,²² combined, indicate a decrease in germ cells, decrease in spermatozoa in semen samples, and IgG deposition in seminiferous tubules in COVID-19, suggesting the existence of humoral immune-mediated injury, as demonstrated by Xu et al. in SARS.²⁰ These studies also reported the loss of spermatogonia through apoptosis²¹⁻²³, the presence of SARS-CoV-2 antigen in interstitial and intratubular cells,²² and viral particles by EM.^{21,22} In the present study, we also demonstrate testes' vascular changes, suggesting ischemia as an alternative mechanism of tissue damage, and the presence of antigens and viral particles in different cell types in the testicular parenchyma, including infection of fibroblasts, which can be associated with tubular fibrosis.

Our study has some limitations. First, we did not present data on patients' semen since they were all in severe clinical condition from the first day of hospitalization. Second, we did not compare our results with a control group. Our study is descriptive, but our findings agree with those of other authors. Our conclusions need to be validated with a more significant number of cases and compared with matched controls. Third, the vessels carrying SARS-Cov-2 infected cells could interfere in the RT-PCR analysis (Figure 3G), rendering false-positive results. However, the IHC was positive in all cases. Moreover, the four cases analyzed under EM showed viral particles in the testicular samples.

The histological study of testicular changes in COVID-19 is essential at this point of the pandemic, as COVID-19 may have affected the fertility and hormonal function of a significant number of men. Interestingly, in the cases presented here, no patient had clinical complaints related to the testicles, suggesting that the lesions are mainly subclinical and that many men may have MRT-related disorders in the future.¹⁵ Prospective studies evaluating the function of the MRT using non-invasive methods (e.g., semen analysis, hormonal status, and Doppler-color ultrasound), with histological correspondence in cases of COVID-19 with different clinical outcomes, may provide helpful answers.

5 | CONCLUSION

In conclusion, we present testicular histological changes in 11 COVID-19 fatal cases including orchitis by mononuclear cells, seminiferous tubule basal membrane thickening, vascular changes (endothelial edema, thrombosis), Leydig cell scarcity, reduced spermatogenesis, and the presence of SARS-CoV-2 antigens and viral particles. These findings may be associated with impaired hormonal function and fertility in men with severe SARS-CoV-2 infection.

ACKNOWLEDGMENTS

The authors wish to thank Kely Cristina Soares Bispo, Cássia Arruda, Thabata Larissa Luciano Ferreira Leite, Catia Sales de Moura, Jair Theodoro Filho, Reginaldo Silva do Nascimento, Adão Caetano, and Dr. Marcelo Alves Ferreira for their technical support. The authors also thank all health workers involved in the care for the patients with COVID-19 and all those that took part in the HC-FMUSP-Coronavirus Crisis Committee during the pandemic.

CONFLICT OF INTEREST

The authors declare that they have no conflict of interest

AUTHOR CONTRIBUTIONS

Amaro N. Duarte-Neto, Jorge Hallak, Katia R. M. Leite, Thiago A. Teixeira, Marisa Dolhnikoff, and Paulo H. N. Saldiva conceived the study. Renata A. A. Monteiro, Paulo H. N. Saldiva, Amaro N. Duarte-Neto, Thais Mauad, Luiz F. F. da Silva, and Marisa Dolhnikoff collected and interpreted the autopsy data. Amaro N. Duarte-Neto and Katia R. M. Leite analyzed and interpreted the testicular pathological findings. Cristina T. Kanamura and Angela B. G. dos Santos carried out IHC and interpreted these together with Amaro N. Duarte-Neto and Katia R. M. Leite. Michele S. Gomes-Gouvêa and João R. R. Pinho performed and interpreted the molecular data. Elia G. Caldini performed and interpreted the EM analysis. Amaro N. Duarte-Neto, Thiago A. Teixeira, Jorge Hallak, Katia R. M. Leite, and Marisa Dolhnikoff prepared the original draft of the manuscript. All authors were involved in writing the paper, and reviewed and approved the final version of the manuscript.

ORCID

Thiago A. Teixeira  <https://orcid.org/0000-0002-6598-2442>

REFERENCES

- Zhou P, Yang XL, Wang XG, et al. A pneumonia outbreak associated with a new coronavirus of probable bat origin. *Nature*. 2020;579:270-273. <https://doi.org/10.1038/s41586-020-2012-7>.
- Wu F, Zhao S, Yu B, et al. A new coronavirus associated with human respiratory disease in China. *Nature*. 2020;579:265-269. <https://doi.org/10.1038/s41586-020-2008-3>.
- Guan WJ, Ni ZY, Hu Y, et al. Clinical characteristics of coronavirus disease 2019 in China. *N Engl J Med*. 2020;382:1708-1720. <https://doi.org/10.1056/NEJMoa2002032>.
- Dong E, Du H, Gardner L. An interactive web-based dashboard to track COVID-19 in real time. *Lancet Infect Dis*. 2020;20:533-534. [https://doi.org/10.1016/S1473-3099\(20\)30120-1](https://doi.org/10.1016/S1473-3099(20)30120-1).
- Gupta A, Madhavan MV, Sehgal K, et al. Extrapulmonary manifestations of COVID-19. *Nat Med*. 2020;26:1017-1032. <https://doi.org/10.1038/s41591-020-0968-3>.
- Teixeira TA, Bernardes FS, Oliveira YC, et al. SARS-CoV-2 and multi-organ damage—what men's health specialists should know about the COVID-19 pathophysiology. *Int Braz J Urol*. 2021;47:637-646. <https://doi.org/10.1590/s1677-5538.ibju.2020.0872>.
- Zou X, Chen K, Zou J, et al. Single-cell RNA-seq data analysis on the receptor ACE2 expression reveals the potential risk of different human organs vulnerable to 2019-nCoV infection. *Front Med*. 2020;14:185-192. <https://doi.org/10.1007/s11684-020-0754-0>.
- Petrilli CM, Jones SA, Yang J, et al. Factors associated with hospital admission and critical illness among 5279 people with coronavirus disease 2019 in New York City: prospective cohort study. *Bmj*. 2020;369:m1966. <https://doi.org/10.1136/bmj.m1966>.
- Richardson S, Hirsch JS, Narasimhan M, et al. Presenting characteristics, comorbidities, and outcomes among 5700 patients hospitalized with COVID-19 in the New York city area. *JAMA*. 2020;323:2052-2059. <https://doi.org/10.1001/jama.2020.6775>.
- Baughn LB, Sharma N, Elhaik E, et al. Targeting TMPRSS2 in SARS-CoV-2 infection. *Mayo Clin Proc*. 2020;95:1989-1999. <https://doi.org/10.1016/j.mayocp.2020.06.018>.
- Wang Z, Xu X. scRNA-seq profiling of human testes reveals the presence of the ACE2 receptor, a target for SARS-CoV-2 infection in spermatogonia, leydig and sertoli cells. *Cells*. 2020;9:920. <https://doi.org/10.3390/cells9040920>.
- Hallak J, Teixeira TA, Bernardes FS, et al. SARS-CoV-2 and its relationship with the genitourinary tract: implications for male reproductive health in the context of COVID-19 pandemic. *Andrology*. 2021;9:73-79. <https://doi.org/10.1111/andr.12896>.
- Illiano E, Trama F, Costantini E. Could COVID-19 have an impact on male fertility? *Andrologia*. 2020;52:e13654. <https://doi.org/10.1111/and.13654>.
- Eisenberg ML. Coronavirus disease 2019 and men's reproductive health. *Fertil Steril*. 2020;113:1154. <https://doi.org/10.1016/j.fertnstert.2020.04.039>.
- Carneiro F, Teixeira TA, Bernardes FS, et al. Radiological patterns of incidental epididymitis in mild-to-moderate COVID-19 patients revealed by colour Doppler ultrasound. *Andrologia*. 2021;53:e13973. <https://doi.org/10.1111/and.13973>.
- Duarte-Neto AN, Monteiro RAA, da Silva LFF, et al. Pulmonary and systemic involvement in COVID-19 patients assessed with ultrasound-guided minimally invasive autopsy. *Histopathology*. 2020;77:186-197. <https://doi.org/10.1111/his.14160>.
- Corman VM, Landt O, Kaiser M, et al. Detection of 2019 novel coronavirus (2019-nCoV) by real-time RT-PCR. *Euro Surveill*. 2020;25:2000045. <https://doi.org/10.2807/1560-7917.ES.2020.25.3.2000045>.
- CDC. (2019-nCoV) Real-time RT PCR primers and probes. Centers for Disease Control and Prevention. 2020. <https://www.cdc.gov/coronavirus/2019-ncov/lab/rt-pcr-panel-primer-probes.html> [Accessed January 27, 2020].
- Hoffmann M, Kleine-Weber H, Schroeder S, et al. SARS-CoV-2 cell entry depends on ACE2 and TMPRSS2 and is blocked by a clinically proven protease inhibitor. *Cell*. 2020;181:271-280.e8. <https://doi.org/10.1016/j.cell.2020.02.052>.
- Xu J, Qi LH, Chi XH, et al. Orchitis: a complication of severe acute respiratory syndrome (SARS). *Biol Reprod*. 2006;74:410-416. <https://doi.org/10.1095/biolreprod.105.044776>.
- Achua JK, Chu KY, Ibrahim E, et al. Histopathology and ultrastructural findings of fatal COVID-19 infections on testis. *World J Mens Health*. 2021;39:65-74. <https://doi.org/10.5534/wjmh.200170>.
- Ma X, Guan C, Chen R, et al. Pathological and molecular examinations of postmortem testis biopsies reveal SARS-CoV-2 infection in the testis and spermatogenesis damage in COVID-19 patients. *Cell Mol Immunol*. 2021;18:487-489. <https://doi.org/10.1038/s41423-020-00604-5>.
- Yang M, Chen S, Huang B, et al. Pathological findings in the testes of COVID-19 patients: clinical implications. *Eur Urol Focus*. 2020;6:1124-1129. <https://doi.org/10.1016/j.euf.2020.05.009>.
- Flaifel A, Guzzetta M, Occidental M, et al. Testicular changes associated with SARS-CoV-2. *Arch Pathol Lab Med*. 2021;145:8-9. <https://doi.org/10.5858/arpa.2020-0487-LE>.
- Reyes JG, Farias JG, Henriquez-Olavarrieta S, et al. The hypoxic testicle: physiology and pathophysiology. *Oxid Med Cell Longev*. 2012;2012:929285. <https://doi.org/10.1155/2012/929285>.
- Teixeira TA, Oliveira YC, Bernardes FS, et al. Viral infections and implications for male reproductive health. *Asian J Androl*. 2021;23:335-347. https://doi.org/10.4103/aja.aja_82_20.
- Gall EA. The histopathology of acute mumps orchitis. *A J Pathol*. 1947;23:637-651.
- Manson AL. Mumps orchitis. *Urology*. 1990;36:355-358. [https://doi.org/10.1016/0090-4295\(90\)80248-I](https://doi.org/10.1016/0090-4295(90)80248-I).
- Jiang Q, Wang F, Shi LL, et al. C-X-C motif chemokine ligand 10 produced by mouse Sertoli cells in response to mumps virus infection induces male germ cell apoptosis. *Cell Death Dis*. 2018;8:e3146. <https://doi.org/10.1038/cddis.2017.560>.

30. Rogers C, Klatt EC. Pathology of the testis in acquired immunodeficiency syndrome. *Histopathology*. 1988;12:659-665. <https://doi.org/10.1111/j.1365-2559.1988.tb01990.x>
31. Bagasra O, Addanki KC, Goodwin GR, et al. Cellular targets and receptor of sexual transmission of Zika virus. *Appl Immunohistochem Mol Morphol*. 2017;25:679-686. <https://doi.org/10.1097/PAL.0000000000000580>
32. Chan JFW, Zhang AJ, Chan CCS, et al. Zika virus infection in dexamethasone-immunosuppressed mice demonstrating disseminated infection with multi-organ involvement including orchitis effectively treated by recombinant type I interferons. *Ebiomedicine*. 2016;14:112-122. <https://doi.org/10.1016/j.ebiom.2016.11.017>
33. Osuna CE, Lim SY, Deleage C, et al. Zika viral dynamics and shedding in rhesus and cynomolgus macaques. *Nat Med*. 2017;22:1448-1455. <https://doi.org/10.1038/nm.4206>
34. Hirsch AJ, Smith JL, Haese NN, et al. Zika Virus infection of rhesus macaques leads to viral persistence in multiple tissues. *PLoS Pathog*. 2017;13:e1006219. <https://doi.org/10.1371/journal.ppat.1006219>
35. Matusali G, Houzet L, Satie AP, et al. Zika virus infects human testicular tissue and germ cells. *J Clin Invest*. 2018;128:4697-4710. <https://doi.org/10.1172/JCI121735>
36. Kawiecki AB, Mayton EH, Dutuze MF, et al. Tissue tropisms, infection kinetics, histologic lesions, and antibody response of the MR766 strain of Zika virus in a murine model. *Viral J*. 2017;14:82. <https://doi.org/10.1186/s12985-017-0749-x>
37. Duarte-Neto AN, Cunha MDP, Marcilio I, et al. Yellow fever and orthotopic liver transplantation: new insights from the autopsy room for an old but re-emerging disease. *Histopathology*. 2019;75:638-648. <https://doi.org/10.1111/his.13904>
38. Duggal NK, Ritter JM, Pestorius SE, et al. Frequent Zika virus sexual transmission and prolonged viral RNA shedding in an immunodeficient mouse model. *Cell Rep*. 2017;18:1751-1760. <https://doi.org/10.1016/j.celrep.2017.01.056>
39. Schindell BG, Webb AL, Kindrachuk J. Persistence and sexual transmission of filoviruses. *Viruses*. 2018;10:683. <https://doi.org/10.3390/v10120683>
40. Martines RB, Ng DL, Greer PW, et al. Tissue and cellular tropism, pathology and pathogenesis of Ebola and Marburg viruses. *J Pathol*. 2015;235:153-174. <https://doi.org/10.1002/path.4456>
41. Baskerville A, Fisherhoch SP, Neild GH, et al. Ultrastructural pathology of experimental ebola hemorrhagic-fever virus-infection. *J Pathol*. 1985;147:199-209. <https://doi.org/10.1002/path.1711470308>
42. Lang ZW. Distribution of hepatitis B virus in testicle tissue in patients with hepatitis B infection. *Zhonghua Yi Xue Za Zhi*. 1993;73:329-331.

How to cite this article: Duarte-Neto AN, Teixeira TA, Caldini EG, et al. Testicular pathology in fatal COVID-19: A descriptive autopsy study. *Andrology*. 2022;10:13-23. <https://doi.org/10.1111/andr.13073>